Journal of Advanced Scientific Research

Available online through http://www.sciensage.info

ISSN 0976-9595

Research Article

SYNTHESIS, CRYSTAL STRUCTURE, HIRSHFELD SURFACE, ENERGY FRAMEWORK, AND MOLECULAR DOCKING ANALYSIS OF DIACRYLATE

G. Dhanalakshmi[1], Jayachandran Karunakaran[2], Arasambattu K. Mohanakrishnan[2], S. Aravindhan*[1]

[1]*Department of Physics, Presidency College (Autonomous), University of Madras, Chennai, Tamilnadu, India*

[2]*Department of Organic Chemistry, University of Madras,Guindy Campus,Chennai, Tamilnadu, India*

**Corresponding author: aravindhanpresidency@gmail.com*

ABSTRACT

The title compound has been synthesized, characterized by ^{1}H NMR,^{13}CNMR, Distortionless Enhancement by Polarization Transfer (DEPT 135 NMR), HR mass spectral analysis, and the structure was confirmed by single crystal X-ray diffraction studies, crystallizes in the triclinic crystal system in P-1 space group with unit cell parameters a = 4.7737(2) Å, b =8.8996(3) Å, c = 10.2405(3) Å, α =88.998(2)°, β =88.137(2)° , γ = 76.316(2)°. The structure has been solved by direct methods and refined by full matrix least squares procedures to a final R value of 0.048 for 1468 observed reflections. The significant difference in the bond lengths is attributed to the partial contribution from the O-_C=O+_C resonance structure of the O1-C7-O2-C8 group. The crystal packing shows the absence of inter-molecular hydrogen bonding. The crystal packing was analyzed using Hirshfeld surfaces method using 2D fingerprint plots and electrostatic potential surfaces. Energy framework calculations were used to analyze and visualize the three dimensional network of the crystal packing. The dispersion energy framework is dominant over the entire energy framework. Molecular docking studies show that the compounds exhibits anti-tumor activity.

Keywords: Crystal structure, Diacrylate, DEPT, HR mass spectra, Hirshfeld surface analysis, Energy framework, Molecular docking

1. INTRODUCTION

Acrylates exhibits anti-bacterial [1], anti-viral, anti-proliferative, anti-atherogenic, anti-oxidant [2], anti-tumour [3], and anti-inflammatory properties [4-6]. Acrylates are used as monomers in the production of adhesives, polymer materials, and as intermediates for heterocycle synthesis [7]. They are used as nitrile-activated precursors in bio reduction reactions [8]. Acrylates does the role of precursors in the synthesis of dye-sensitized photovoltaic materials [9-11] and sensors [12]. Acrylate compounds are used in the synthesis of quinoline-3-carbonitrile derivatives, which are used for the treatment of rheumatoid arthritis [13-14].

Acrylate resins are widely used in coating applications [15-18]. They also provide remarkable Anti-bacterial and self cleaning properties [19-22]. Methyl acrylate is an ester of acrylic acid. It is an important polymer that can be used in various industrial applications [23]. It is used in the production of elastomers, fibers, coatings, paints, and inks [24, 25].Polyurethane-acrylate (PUA) composite materials have good abrasion resistance, corrosion resistance, water resistance, and weather resistance. Their preparation protocol is cost-effective, requires low-energy consumption, and involves no solvent pollution. PUA is widely used in the coating industry, textile industry, construction industry, and several other [26- 31]. In recent times, the study of polyurethane acrylate composite emulsions has gained increasing attention from a large number of researchers. In this present study, we report the synthesis, ^{1}H,^{13}C NMR, DEPT 135 NMR, High resolution mass spectral analysis, single crystal X-ray diffraction studies, Hirshfeld surface, Energy framework, and Molecular docking analysis of a novel compound Diethyl 3,3'-(2,5-dimethyl-1,4-phenylene)(2E,2'E)-diacrylate.

2. MATERIAL AND METHODS

2.1. Synthesis of title compound

To a stirred solution of 2,5-dimethylterephthalaldehyde 1 (0.20 g, 1.23 mmol) in dry DCM, stabilized Wittig ylide (1.07 g, 3.07 mmol) was added and the reaction mixture was stirred at room temperature for 5 h under N_2 atmosphere. After completion of reaction (monitored by TLC) solvent was removed under reduced pressure

followed by titration with methanol to give Diethyl 3,3'-(2,5-dimethyl-1,4-phenylene)(2E,2'E)-diacrylate 2 as a (0.26 g, 70%) colorless solid. MP 104-106 °C. ^{1}H, ^{13}C and DEPT 135NMR spectra were recorded in $CDCl_3$ using TMS as an internal standard on Bruker 300 MHz spectrometer at room temperature.

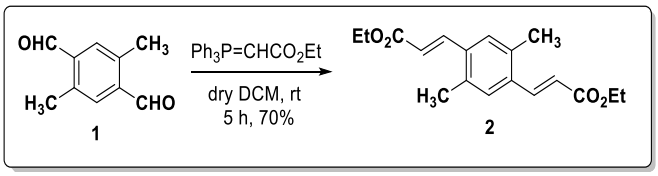

Reaction Scheme: Wittig Reaction

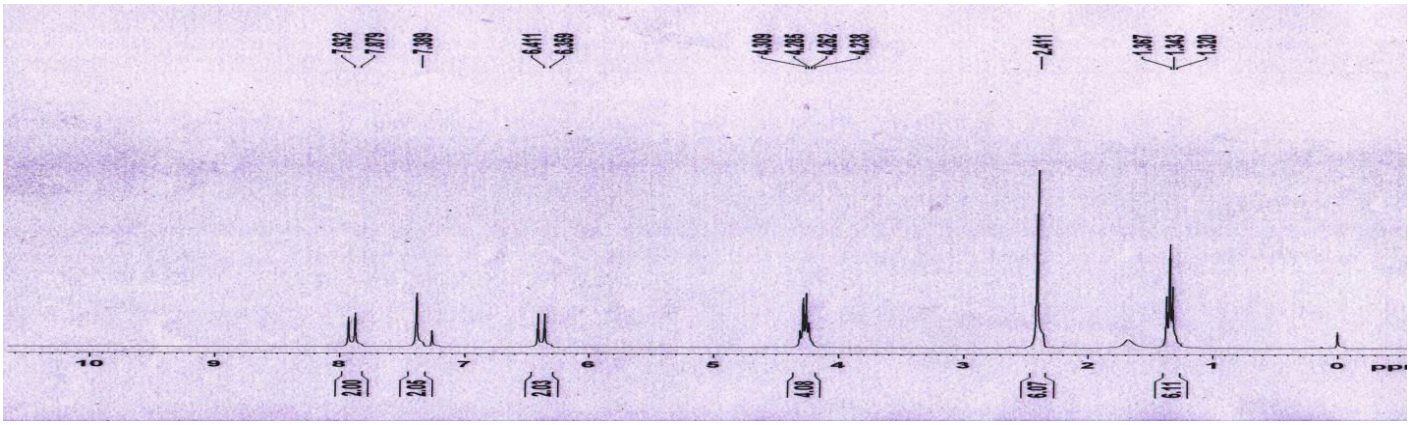

Fig. 1: ^{1}H-NMR spectrum of the title compound

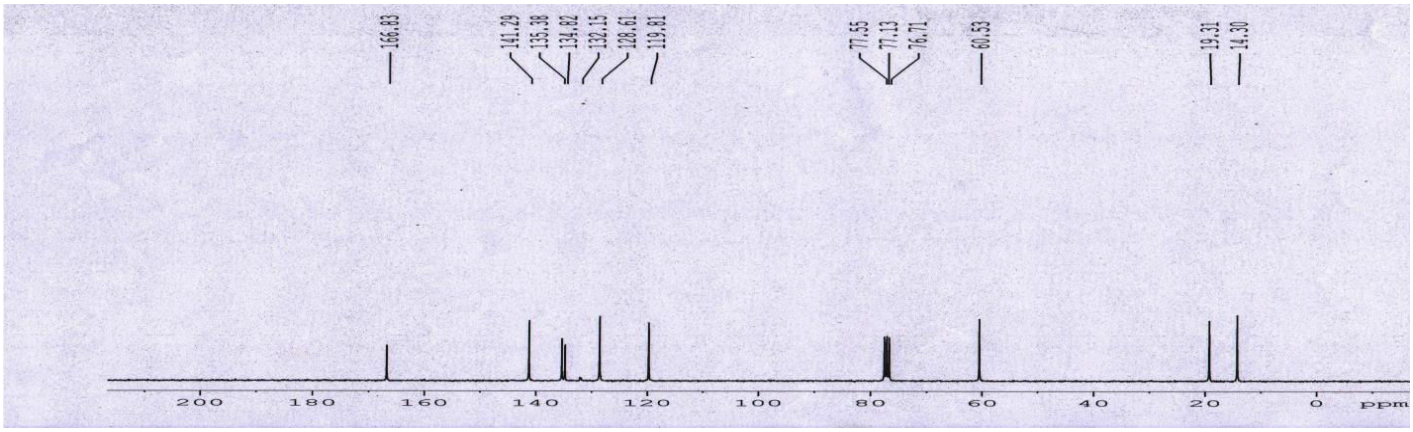

Fig. 2: ^{13}C-NMR spectrum of the title compound

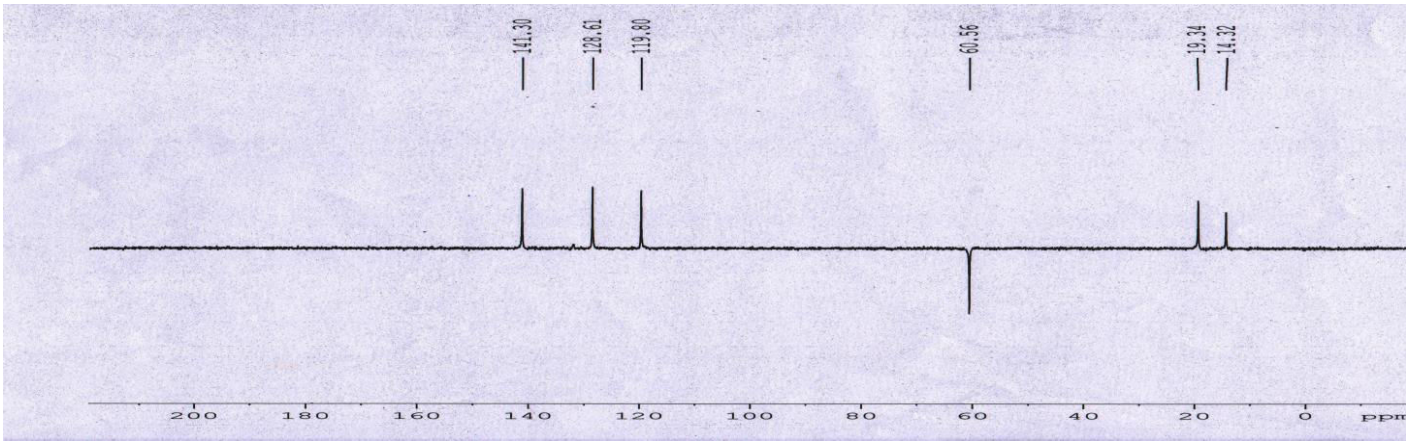

Fig. 3: DEPT 135-NMR spectrum of the title compound

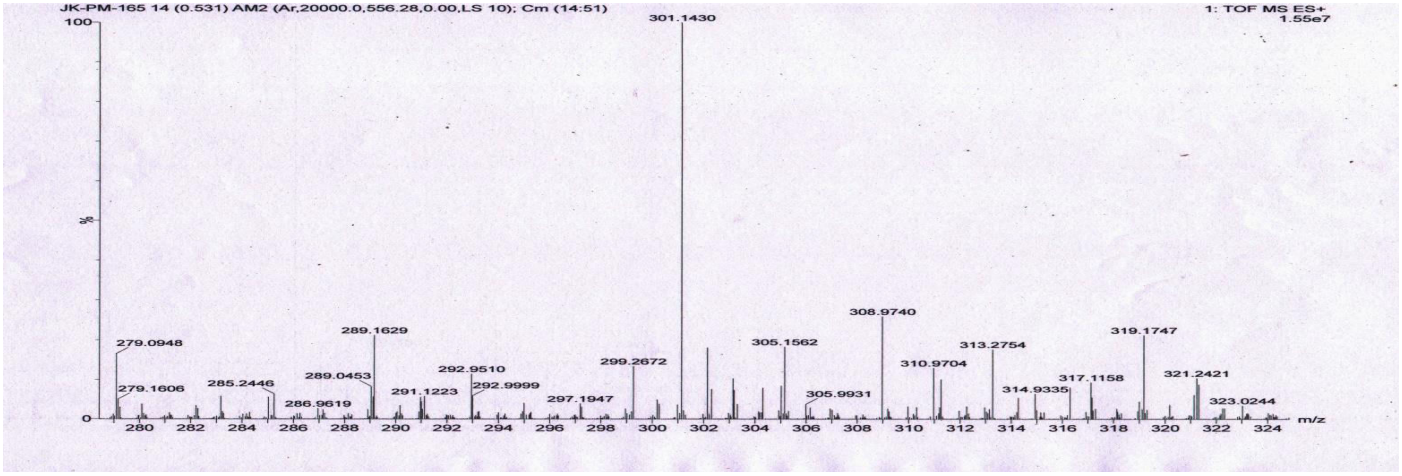

Fig. 4: HRMS Spectrum of the title compound

Chemical shift values were quoted in parts per million (ppm) and coupling constants were quoted in hertz (Hz). HRMS were recorded on Xevo G2S QTof (ESI) instrument.1H-NMR (300 MHz, CDCl3): δ 7.91 (d, J = 15.9 Hz, 2H, vinyl C-H), 7.39 (s, 2H, ArH), 6.39 (d, J = 15.6 Hz, 2H, ArH), 4.27 (q, J = 14.1 Hz, 4H, OCH2), 2.41 (s, 6H, Ar-CH3), 1.34 (t, J = 7.0 Hz, 6H, CH3) ppm. 13C-NMR (75 MHz, CDCl3): δ 166.8, 141.3, 135.4, 134.8, 132.2, 128.6, 119.8, 60.5, 19.3, 14.3 ppm. DEPT 135-NMR (75 MHz, CDCl3): δ 141.3, 128.6, 119.8, 60.6, 19.3, 14.3 ppm; HRMS (ESI-TOF) m/z: [M-H]+ calcd for $C_{18}H_{22}O_4$: 301.1440, found: 301.1430.^{1}H NMR,^{13}C-NMR,DEPT 135-NMR and HR mass spectrum of the title compound are as shown in the Fig. 1-4.

2.2. Single Crystal X-ray Diffraction studies

Single crystals of the size 0.200 x 0.150 x 0.100 ^{mm3} were taken for X-ray diffraction study using a Bruker axs kappa Apex2 CCD Diffractometer at 296K with graphite monochromatic MoK$_\alpha$ radiation of wavelength (λ)= 0.71073 Å. Data were corrected for Lorentz-polarization and absorption factors. The structure was solved by direct methods using SHELXT-2014/4 [32], and refined using *SHELXL2014*/7 [33], by full matrix least squares on F^2. All non-hydrogen atoms were refined anisotropically and H atoms were localized from the difference electron-density maps and refined as riding atoms with C-H = 0.93 or 0.97 Å with U_{iso}(H) = 1.5U_{eq}(C) for methyl H atoms and 1.2U_{eq}(C) for other H atoms. The geometrical calculations were carried out using the program *PLATON* [34]. The molecular and packing diagrams were generated using the software *MERCURY* [35].

2.3. Hirshfeld surface analysis

Hirshfeld surface analysis [36-37] and fingerprint plots [38-39] has been used to analyze the different intermolecular interactions [40-41]. Hirshfeld surface analysis was carried out using Crystal Explorer version 17.0 [42]. TONTO [43] combined within Crystal Explorer was used to calculate the electrostatic potentials. The STO-3G basis set at the HF level of theory over the range 0.03 au was used to map the electrostatic potential on the Hirshfeld surface. The d_{norm} and curvedness plots were mapped on Hirshfeld surface [0.364 au (blue) to 1.2842 au (red)) and (-4.00 au to 0.400 au)]. The red and blue colour on the d_{norm} represents the shorter and longer inter contacts, and the white colour indicates the contacts around the vander Waals radii [44, 45]. The 2D fingerprint plots were drawn in the range of 0.6-2.8 Å where d_i is the closest internal distance and d_e is the closest external distance from a given point on the Hirshfeld surface.

3. RESULTS & DISCUSSION

3.1. Single crystal X-ray diffraction

The compound C_{18} H_{22} O_4 crystallizes in the crystal system triclinic with P-1 space group. Out of 10798 reflections collected, 1468 reflections were found to be independent and 102 parameters were refined. The structure was solved to final R1 indices value of 0.0475. The Goodness of fit on $F^2$was found to be 1.054. The largest difference peak and hole was found to be 0.120 and -0.136e Å^{-3}. The cell parameters of the title compound are a = 4.7737(2) Å, b =8.8996(3) Å, c = 10.2405(3) Å, α =88.998(2)°, β =88.137(2)° , γ =76.316(2)°, Z = 1,and V= 422.46(3) Å^3. The ORTEP diagram of the title compound with

displacement ellipsoids drawn at the 40% probability level is shown in Fig. 5. The crystal data and structure refinement details are given in Table 1.

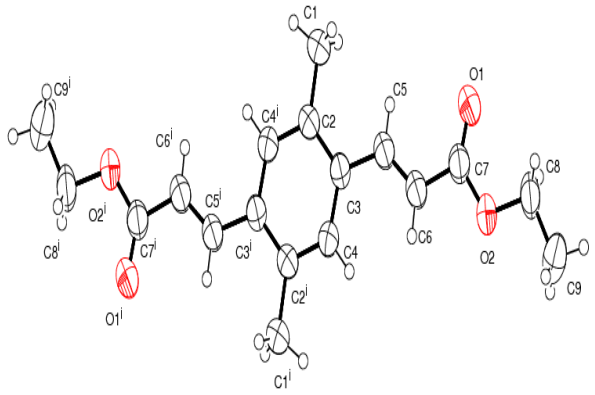

Fig. 5: The ORTEP diagram of the title compound with the atom labeling.

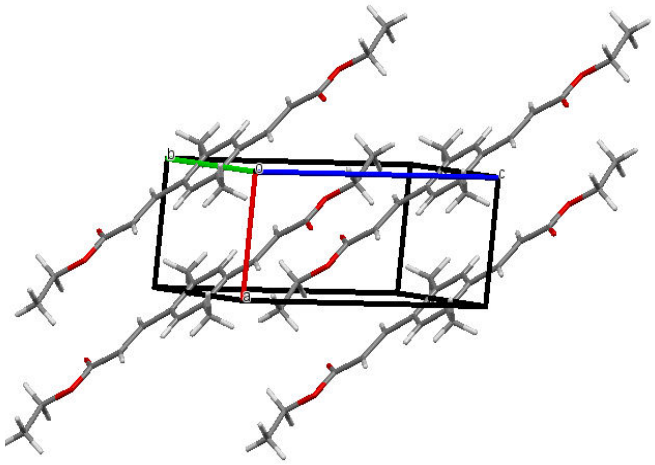

Fig. 6: The crystal packing of title compound viewed along the b axis, showing the absence of intermolecular hydrogen bonds

The molecular structure consists of phenyl ring substituted with methyl acrylate at 2, and 5 positions. In the title molecule, the acrylate unit is planar, with a maximum deviation of 0.036(2) Å for atom C8 and forms a dihedral angle of 2.66(9) º with the phenyl ring (C2-C4a).The values of bond lengths and angles agree with those observed in literature [46]. The torsion angles for O2-C7-C6-C5 and O1-C7-C6-C5 are -175.34(18) º and 4.3(3)º respectively which indicates they are (-) anti-periplanar and (+) syn-periplanar with the phenyl ring. The difference in the bond lengths O2-C8=1.444(2) Å and O2-C7=1.333(2) Å are due to the partial contribution from the O^-_C=O^+_C resonance structure of the O1-C7-O2-C8 group [47]. The crystal packing shows the absence of inter-molecular hydrogen bonding.(Fig 6)

Table 1: Crystal data and structure refinement for title compound

PARAMETER	VALUE
CCDC NO	1858371
Empirical formula	C18 H22 O4
Formula weight	302.35
Temperature	293(2) K
Wavelength	1.54178 Å
Crystal system	Triclinic
Space group	P-1
Unit cell dimensions	a = 4.7737(2) Å a= 88.998(2)°
	b = 8.8996(3) Å b= 88.137(2)°
	c = 10.2405(3) Å c =76.316(2)°.
Volume	422.46(3) Å3
Absorption coefficient	0.674 mm-1
F(000)	162
Crystal size	0.200 x 0.150 x 0.100 mm3
Theta range for data collection	4.320 to 65.968°.
Index ranges	-5<=h<=5, -10<=k<=10, -12<=l<=12
Reflections collected	10798
Independent reflections	1468 [R(int) = 0.0598]
Completeness to theta = 65.968°	99.50%
Absorption correction	Semi-empirical from equivalents
Max. and min. transmission	0.7536 and 0.6343
Refinement method	Full-matrix least-squares on F2
Data / restraints / parameters	1468 / 0 / 102
Goodness-of-fit on F2	1.054
Final R indices [I>2sigma(I)]	R1 = 0.0475, wR2 = 0.1188
R indices (all data)	R1 = 0.0712, wR2 = 0.1337
Largest diff. peak and hole hole	0.120 and -0.136 e.Å-3

Table 2: Bond lengths [Å] for Compound

Bond	Bond length [Å]
C(1)-C(2)	1.507(2)
C(2)-C(4)#1	1.383(2)
C(2)-C(3)	1.402(2)
C(3)-C(4)	1.393(2)
C(3)-C(5)	1.462(2)
C(4)-C(2)#1	1.383(2)
C(5)-C(6)	1.303(3)
C(6)-C(7)	1.465(2)
C(7)-O(1)	1.186(2)
C(7)-O(2)	1.333(2)
C(8)-O(2)	1.444(2)
C(8)-C(9)	1.486(3)

Table 3: Selected Torsion angles [Å] for Compound

Bond	Bond angle[Å]
C(1)-C(2)-C(3)-C(4)	-178.68(18)
C(4)#1-C(2)-C(3)-C(5)	179.63(16)
C(5)-C(3)-C(4)-C(2)#1	-179.64(17)
C(2)-C(3)-C(5)-C(6)	178.80(19)
C(3)-C(5)-C(6)-C(7)	179.28(17)
C(5)-C(6)-C(7)-O(2)	-175.33(18)
C(6)-C(7)-O(2)-C(8)	178.39(16)
C(9)-C(8)-O(2)-C(7)	174.82(17)

Table 4: Selected bond angles [Å] for Compound

Bond	Bond angle[Å]	Bond	Bond angle[Å]
C(2)-C(1)-H(1A)	109.5	C(7)-C(6)-H(6)	118.5
C(4)#1-C(2)-C(3)	118.02(15)	O(1)-C(7)-O(2)	122.47(17)
C(4)#1-C(2)-C(1)	119.81(16)	O(1)-C(7)-C(6)	126.18(18)
C(3)-C(2)-C(1)	122.16(15)	O(2)-C(7)-C(6)	111.34(15)
C(4)-C(3)-C(2)	118.38(15)	O(2)-C(8)-C(9)	107.74(17)
C(4)-C(3)-C(5)	120.69(15)	O(2)-C(8)-H(8A)	110.2
C(6)-C(5)-H(5)	116	H(8A)-C(8)-H(8B)	108.5
C(5)-C(6)-C(7)	123.05(17)	C(8)-C(9)-H(9A)	109.5
C(5)-C(6)-H(6)	118.5	C(7)-O(2)-C(8)	116.83(15)

3.2. Hirshfeld Surface

The volume inside the Hirshfeld surface is 414.59 $Å^3$ with an area of 397.14 $Å^2$ .The globularity (G), and asphericity values are 0.677and 0.519 respectively. The non-appearance of red spot in $d_{norm.}$ (Fig. 7a) confirms the absence of inter-molecular contacts which justifies the xrd results. The blue region of electrostatic potential (Fig 7b) denotes positive electrostatic potential and the red region denotes negative electrostatic potential. The absence of red-blue triangle and the flat region on the curvature (Fig.8a and Fig.8b) shows the absence of π…π stacking interactions which substantiates the X-ray diffraction result.

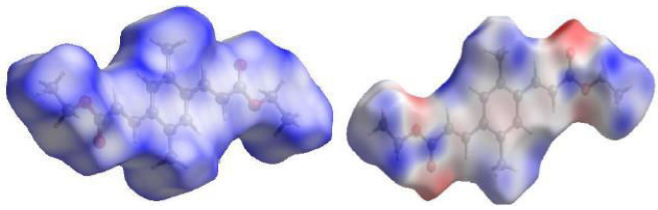

Fig. 7: View of the Hirshfeld surface mapped over a) d_{norm} and b) electrostatic potential

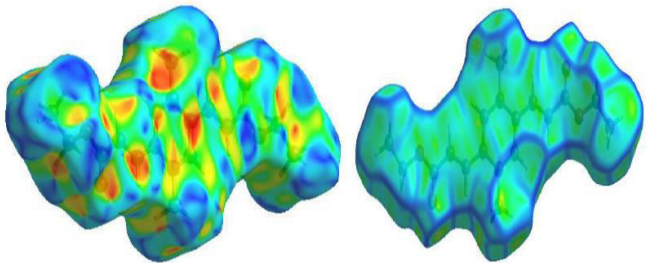

Fig.8: Hirshfeld surface mapped with a) shape index b) curvature

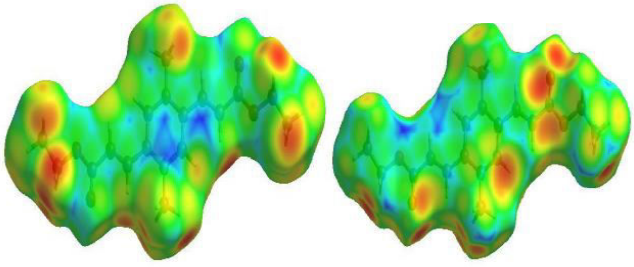

Fig.9: Hirshfeld surface mapped with a) d_i and b) d_e

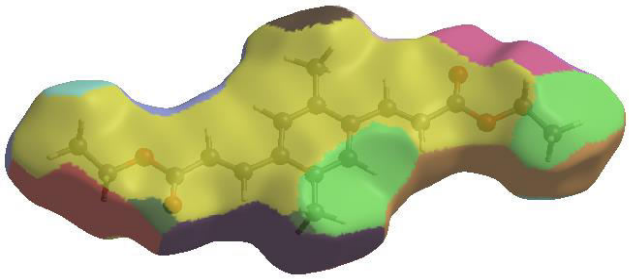

Fig. 10: d $_{norm}$ mapped over the hirshfeld surface showing the Fragment patches

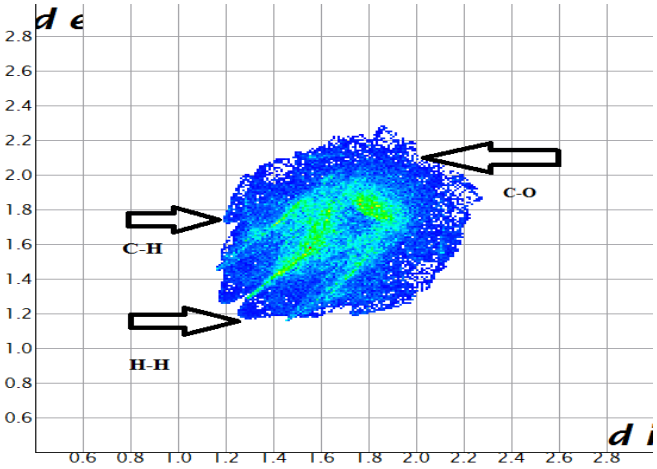

Fig. 11: 2D Fingerprint plots showing the overall interactions

Fig. 9a and 9b shows the Hirshfeld surface mapped over d_i and d_e . The colour patches on the Hirshfeld surface depicts the closest neighbour coordination environment of a molecule (Fig. 10)The full two-dimensional fingerprint plot,is shown in Fig.11 and H…H, C…H/H…C, C…O/O…C interactions are illustrated in Fig.12. The H…H interactions is the highest with a contribution of 59.6% of Hirshfeld Surface. The C…H/H…C interactions appear as two wings, which is represented by inverted umbrella shape with a contribution of 1.6% of the Hirshfeld surfaces.

3.3. Energy framework Analysis

The four components electrostatic, polarization, dispersion and exchange repulsion expresses the interaction energy between the molecules. These energies were obtained using monomer wave functions calculated at the HF/3-21G level. The total interaction energy, which is the sum of scaled components, was calculated for a 3.8 A° radius cluster of molecules around the selected molecule (Fig.13a). The interaction energies calculated by the energy model discloses that the interactions in crystal have a important contribution from dispersion components of the title compound (Table 5). The magnitudes of the intermolecular interaction energies are represented graphically using energy frameworks and the supramolecular architecture of the crystal structures are shown in Fig 13b-13d .The total interaction energies are electrostatic (E_{ele} =-26.3 kJ mol^{-1}), polarization (E_{pol} = -13.1 kJ mol^{-1}),dispersion (E_{dis} = -168.3 kJ mol^{-1}), repulsion (E_{rep} =60 kJ mol^{-1}), and total interaction energy (E_{tot} =-138.2 kJ mol^{-1}). The dispersion energy framework is dominant over all other energy frameworks.

Table 5: Interaction energies (kJ mol^{-1}) for the title compound between a reference molecule and its neighbours

N	Symop	R	Electron Density	E_ele	E_pol	E_dis	E_rep	E_tot
2	x, y, z	17.49	HF/3-21G	-5.0	-1.8	-11.8	5.3	-12.6
2	x, y, z	13.77	HF/3-21G	1.1	-1.3	-17.4	5.6	-10.8
2	x, y, z	11.16	HF/3-21G	0.2	-0.5	-18.2	5.1	-12.3
2	x, y, z	4.77	HF/3-21G	-5.4	-2.7	-85.8	31.4	-59.2
2	x, y, z	8.90	HF/3-21G	-9.0	-4.2	-17.7	8.8	-20.7
2	x, y, z	11.05	HF/3-21G	-1.9	-0.6	-3.7	0.0	-5.6
2	x, y, z	14.85	HF/3-21G	-6.4	-1.8	-9.3	3.1	-13.5
2	x, y, z	9.05	HF/3-21G	0.1	-0.2	-4.4	0.7	-3.5

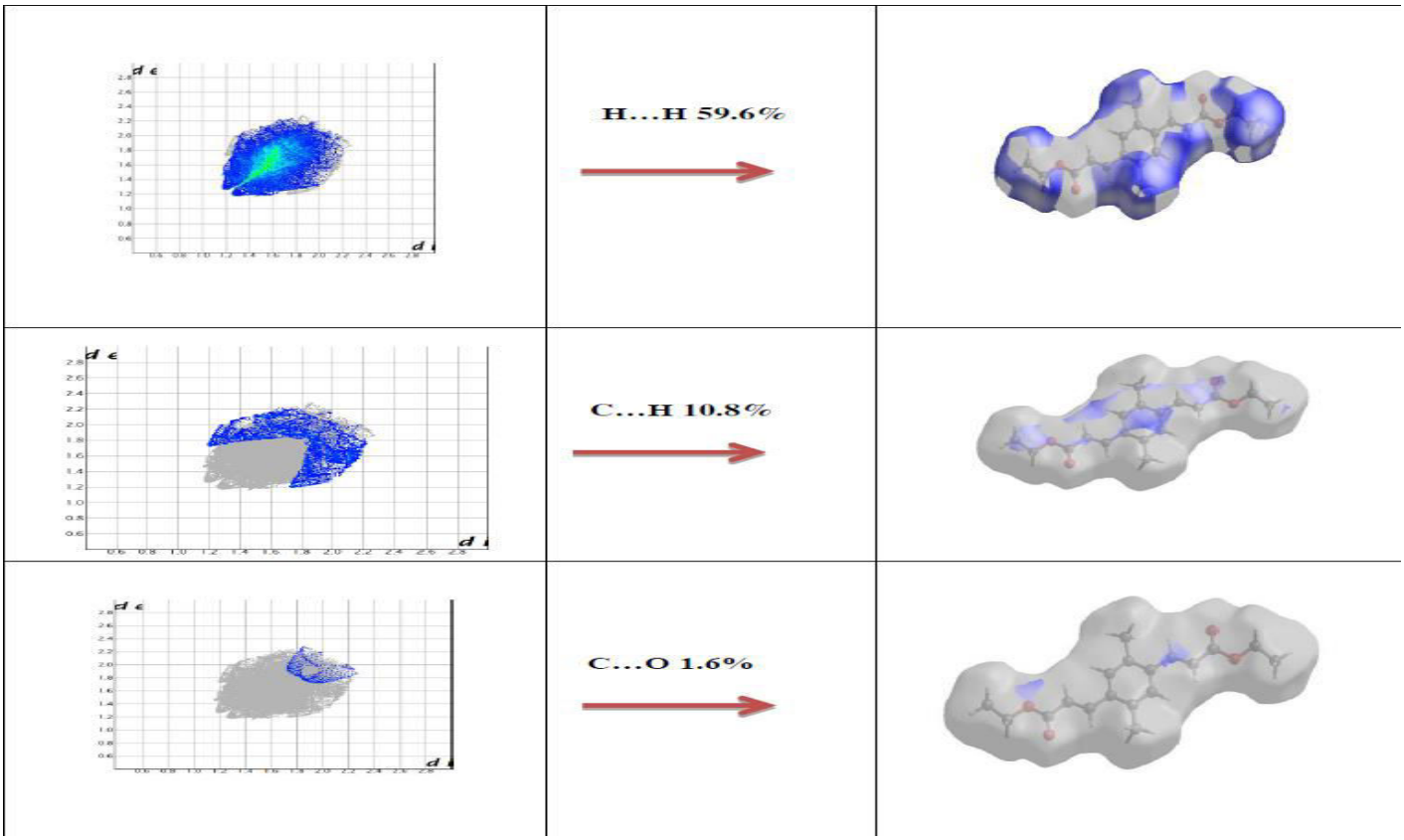

Fig. 12: 2D- Finger print with d_{norm} surface view of the title compound

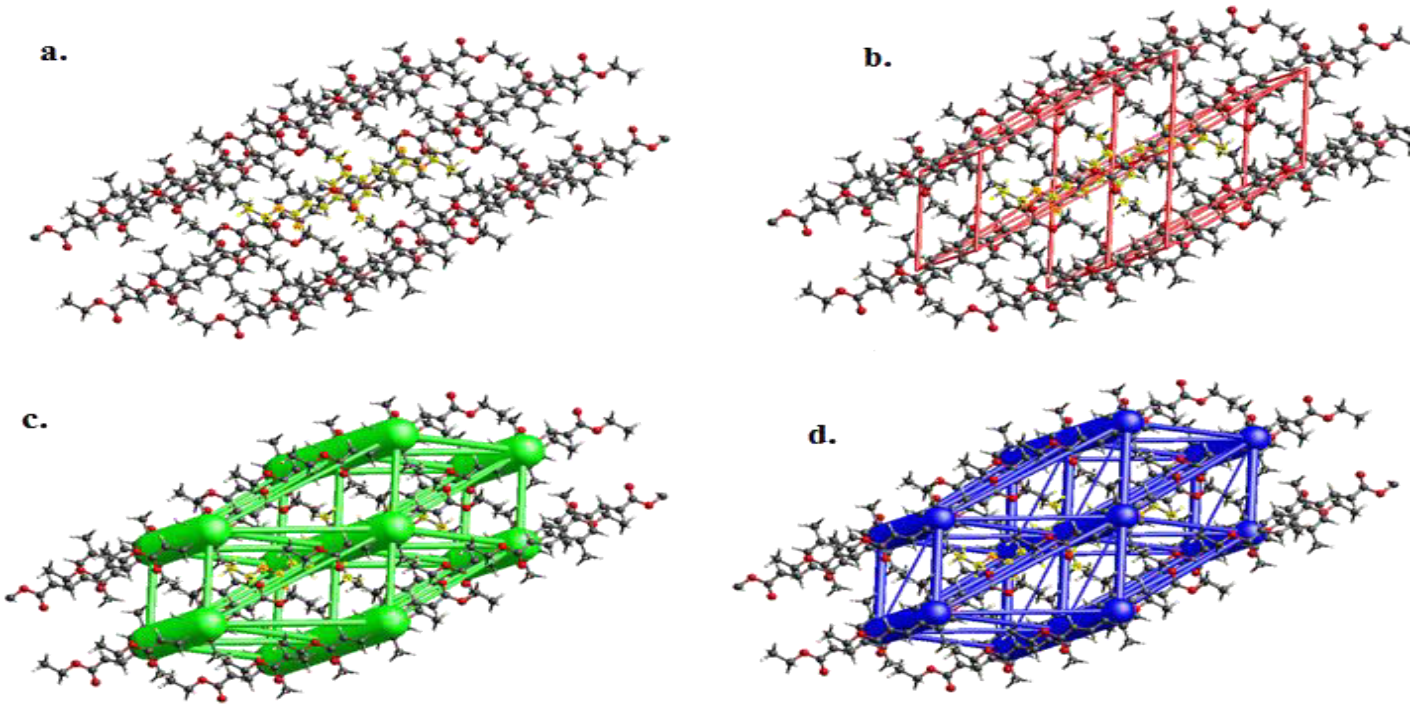

Fig. 13: (a) Interactions between the selected reference molecule (highlighted in yellow) and the molecules present in a 3.8 Å cluster around it, (b) Coulomb energy framework, (c) dispersion energy framework and (d) total energy framework

3.4. Molecular Docking studies

The thioredoxin system, composed of thioredoxin reductase (TrxR), thioredoxin (Trx), and NADPH, is a highly conserved, ubiquitous network in all cells, and plays crucial roles in the redox regulation of numerous cellular signaling pathways involved in cell survival and proliferation [48-50].In recent years, accumulating evidence supports that TrxR is a promising target for development of novel anticancer agents as the thioredoxin system is often overexpressed in many tumors [51] and this over expression confers drug resistance in cancer chemotherapy[52].

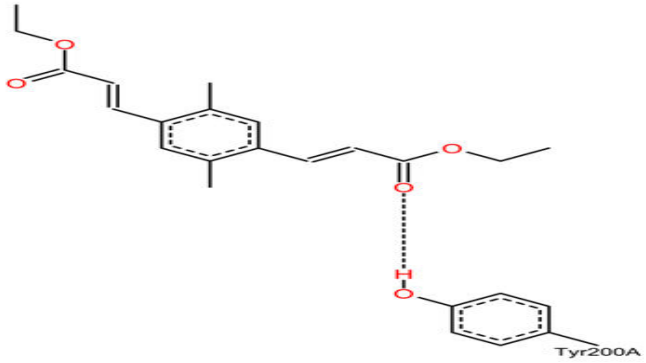

Fig. 14: Poseview diagram of the title compound

The PDB file about the Structure of Human Thioredoxin Reductase 1 (PDB ID: 2J3N)[53] was obtained from the RCSB protein data bank (http://www.pdb.org). The molecular docking procedure was performed by using Autodock docking software [54]. For ligand preparation, the 3D structure of Diacrylate was optimized with B3LYP/DFT method. The active site contains the highly conserved residues 18ILE, 19GLY, 20GLY, 21GLY, 22SER, 23GLY, 24GLY, 41LEU, 42ASP, 43PHE, 44VAL, 45THR. Analyses of hydrogen-bond interactions confirmed that Tyr200A play the relatively important role in binding potency. The energy value between Diacrylate and Thioredoxin reductase is -3.52kcal/mol. The Distance of hydrogen bond formed between Protein and ligand is 2.3Å.

4. CONCLUSION

The title compound Diethyl 3,3'-(2,5-dimethyl-1,4-phenylene)(2E,2'E)-diacrylate 2 has been synthesized. The compound hasbeen characterized using the ^{1}H, ^{13}C NMR, DEPT 135 NMR, HR mass spectrum. The molecular structure of the compound was confirmed by the single crystal X-ray diffraction studies. The crystal packing shows the absence of inter-molecular hydrogen bonding. Hirshfeld surface analysis and fingerprint plots provide the percentage contribution from each individual contact. Energy framework analysis shows that the dispersion energy framework is dominant over all other energy frameworks.. Molecular docking studies show that the compounds exhibits anti-tumor activity.

5. ACKNOWLEDGEMENTS

The authors wish to acknowledge the SAIF, IIT, Madras for the data collection

6. SUPPLEMENTARY DATA

Crystallographic data for the structural analysis have been deposited with the Cambridge crystallographic Data Center,CCDC reference numbers: 1858371.Copies of thisinformation may be obtained free of the charge from the Director, CCDC, 12 Union Road, Cambridge, CB2 1EZ, UK,(Fax: +44-1223-336033; E-mail: deposit@ ccdc.cam.ac.uk or http://www.ccd.cam.ac.uk).

Conflict of Interest

The authors declare no conflict of interests

7. REFERENCES

1. Xiao ZP, Fang RQ, Li HQ, Xue JY, Zheng Y, Zhu HL. *Euro. J. medi. chem.,* 2008; **43(9)**:1828-1836.
2. Uwai K, Osanai Y, Imaizumi T, Kanno SI, Takeshita M, Ishikawa M. *Bio. & Med. Chem.,* 2008; **15(16)**:7795-7803.
3. DeCamposBuzzi F, Franzoi CL, Antonini G, Fracasso M, CechinelFilho V, Yunes RA, Niero R. Eur. J. Med. Chem., 2009; **44(11)**:4596-602.
4. Ates B, Dogru M I, Gul M. *Fund. Clin. Pharma.*, 2006; **20**:283-289.
5. Atik E, Goeruer S, Kiper AN. *Pharma. Res*, 2006; **54:**293-297.
6. Padinchare R, Irina V, Paul C, Dirk VB, Koen A, Achiel H. *Bio.org. Med. Chem. Lett.*, 2001; **11**:215-217.
7. Gololobov YG, Krylova T. *Hetero. Chem.*, 1995; **6:**271-280.
8. Winkler C, Clay D, Turrini N, Lechner H, Kroutil W, Davies S, et al. *Adv. Synth. Catal.,* 2014; **356**:1878-1882.
9. Chen C, Yang X, Cheng M, Zhang F and Sun L. *Chem.Sus.Chem.*, 2013; **6**:1270-1275.

10. Zietz B, Gabrielsson E, Johansson V, El Zohry A, Sun L, Kloo L. *Phys. Chem. Chem. Phys.*, 2014; **16**:2251-2255.
11. Lee M, Cha SB, Yang S, Woong Park, Kim K, Park N, Lee D. *Kor.Chem. Soc.,* 2009; **30**:2260-2279.
12. Zhang X, Yang Z, Chi Z, Chen M , Xu B, Wang C, et al. *J. Mater. Chem.*, 2010; **20**:292-298.
13. Zhang SL, Zhai X, Zhang SJ, Yu HH, Gong P. *Chinese.Chem.Lett*., 2010; **21**:939-942.
14. Hu YH, Green N , Gavrin GL . *Bioorg. Med. Chem*., 2006; **16**:6067-6072.
15. Nguyen TV, Le XH, Dao PH, Decker C.2018; **124:**137-146.
16. Decker C, Masson F, Schwalm R. *Poly. Degrad. and Stab.*, 2004; **83(20):**309-320.
17. Decker C, Zahouily K., *Poly. Degrad. and Stab.*, 1999; **64(2)**:293-304.
18. Nguyen TV, Tri PN, Nguyen TD, El Aidani R, Decker C. *Poly. Degrad. and stab.*, 2008; **128**:65-76.
19. Nguyen TN, Do LN, Guyen TV, Dao TV, Nguyen PH, Dinh AH, Le DA. *Prog. in Org.Coat*., 2009; **132**:15-20.
20. Barani H. *App. Sur.sci.,* 2014; **320**:429-434.
21. Ngo TD, Le T, Nguyen MH, Nguyen TV, Le TA, Nguyen TL, Doan NH. *Inter. J. Poly. Sci.,* 2016; 352-362.
22. Nguyen TV, Do TV, Ha MH , Le HK, Le TT, Nguyen TNL, NguyenTri P. *Pro. in Org. Coat.,* 2020; **139:**105325.
23. Nain, Anil Kumar. *The J. of Chem. Thermo.,* 2013; **60**:105-116.
24. Nain, Anil Kumar. *Fl. Ph. Equi*., 2008; **265(1-2)**:46-56.
25. Chowdary N, Nain AK. *J. Mol. Liquid.,* 2018; 501-513.
26. Du S,Wang Y, Zhang C, Deng X, Luo X, Fu Y, Liu Y. *J. Mater. Sci*, 2018; **53**:215-229.
27. Turri S, Levi M, Trombetta T. *Macro Symp*, 2009; **218**:29-38.
28. Asif A, Hu L, Shi W. *Colloid. Polym. Sci.*, 2009**;** **287**:1041-1049.
29. Lee BS, Chun BC, Chung YC, Sul KI, Cho JW . *Macro.*, 2001; **34**:6431-6437.
30. Wang C, Li X, Du B, Li P, Lai X, Niu Y. *Colloid Polym Sci.,* 2014; **292**:579-587.
31. Ma, Le, Lina Song, Fang Li, Heng Wang, and Baohua Liu. *Coll. and Poly. Sci,* 2017; **295(12):** 2299-2307.
32. Sheldrick GM. *Acta Cryst.* A,2015a; **71**:3-8.
33. Sheldrick GM. *Acta Cryst.,* C,2015b; **71**:3-8.
34. Spek AL. *Acta Cryst.,* 1990; **A46**:c34.
35. Macrae CF, Bruno IJ , Chisholm JA, Edgington PR, McCabe P, Pidcock E, Rodriguez LM , et al. *J. Appl. Cryst*. 2008; **41**:466-470.
36. Spackman MA, Jayatilaka D. *Cryst. Engg. Comm.,* 2009; **11**:19-32.
37. Spackman MA, McKinnon MJ . *Cryst. Engg. Comm.,* 2009; **4**:378-392
38. Spackman MA. *Phys. Scr.,* 2013; **87**:1-12.
39. McKinnon MA, Spackman AS, Mitchell. *Struct. Sci.,* 2004; **60**:627-668.
40. Seth SK, Sarkar D, Roy A, Kar T. *Cryst Eng Comm*., 2011; **13**:6728-6741.
41. Seth SK. *Inorg. Chem. Commun*., 2014; **43**:60-63.
42. Turner MJ, McKinnon JJ, Wolff SK, Grimwood DJ, Spackman PR, Jayatilaka D, Spackman MA. *CrystalExplorer.*,2017; The University of Western Australia.
43. Jayatilaka D, Grimwood DJ, Lee A, Lemay A, Russel AJ, Taylor C, Wolff SK, Cassam-Chenai, Whitton P. 2005;TONTO. http://hirshfeldsurface.net
44. Kumara K, Harish KP, Naveen S, Tandon HC, Mohana KN, Lokanath NK. *Chem.Data Coll*., 2017; **11-12**:40-58.
45. Kumara K, Jyothi M, Naveen S, Zabiulla SA, Khanum NK, Lokanath. *Chem. DataColl*., 2017;**9-10:**152-163.
46. Wang L, Meng FY, Lin CW, Chen HY, Luo X. *Acta Cryst.,* 2011; **E67:**o354.
47. Merlino S, *Acta Cryst.*,1971; **B27:** 2491-2492.
48. Varghese B, Srinivasan S, Padmanabhan PV, Ramadas SR. *Acta Cryst.*,1986; **C42**:1544-1546.
49. Mahmood DF, Abderrazak A, Khadija EH, Simmet T, Rouis M. *Anti. Redox. Sig.,* 2013; **19**:1266-1303.
50. Bindoli A, Rigobello MP. *Antioxid. Redox Signal*. 2013; **18**:1557-1593.
51. Kahlos K, Soini Y, Saily M, Koistinen P, Kakko S, Paakko P, Holmgren A, Kinnula VL. *Int. J. Can,* 2001; **95:**198-204.
52. Berggren M, Gallegos A, Gasdaska JR, Gasdaska PY, Warneke J, Powis G. *Anticancer Res*. 1996; **16**:3459-3466.
53. Kim SJ, Miyoshi Y, Taguchi T, Tamaki Y, Nakamura H, Yodoi J. *Clin. Cancer Res*. 2005: **11:**8425-8430.
54. Karin Fritz-Wolf1, Sabine Urig, Katja Becker. *J. Mol. Biol*. 2007; **370**:116-127.